Interaction network structure explains species temporal persistence in empirical plant-pollinator communities

Virginia Domínguez-Garcia[1]*, Francisco P. Molina[1], Oscar Godoy[2] and Ignasi Bartomeus[1]

[1]Estación Biológica de Doñana (EBD-CSIC), Seville, Spain
[2]Departamento de Biología, Instituto Universitario de Ciencias del Mar (INMAR), Universidad de Cádiz, Puerto Real, Spain
*corresponding author: Virginia domínguez García domgarvir@gmail.com, virginia.dominguez@ebd.csic.es

Despite clear evidence that some pollinator populations are declining, our ability to predict pollinator communities prone to collapse or species at risk of local extinction is remarkably poor. Here, we develop a model grounded in the structuralist approach that allows us to draw sound predictions regarding the temporal persistence of species in mutualistic networks. Using high-resolution data from a 6-year study following 12 independent plant-pollinator communities, we confirm that pollinator species with more persistent populations in the field are those theoretically predicted to tolerate a larger range of environmental changes. Persistent communities are not necessarily more diverse, but are generally located in larger habitat patches, and present a distinctive combination of generalist and specialist species resulting in a more nested structure, as predicted by previous theoretical work. Hence, pollinator interactions directly inform about their ability to persist, opening the door to use theoretically informed models to predict species' fate within the ongoing global change.

Pollinators are key components of ecological systems that provide a wide variety of ecosystem functions and services critical for human well-being, such as plant reproduction[1] and food security[2]. However, the maintenance of these functions is at risk due to the ongoing negative effects of global change drivers on pollinator abundance and diversity[3, 4, 5]. There have been several calls to face the global crisis of pollinator decline by providing tools that accurately predict their population dynamics, and therefore their probability of extinction[6], however, our ability to achieve a predictive ecology is still limited [7]. The need to predict, and hence to understand, how ecological communities respond to ongoing environmental changes has historically fueled intense research on ecological stability[8, 9, 10]. Yet, this research has been hampered by both a profound divide between the theoretical and the empirical studies[11, 10, 12], and an unclear definition of the concept of ecological stability itself[10, 13]. This still ongoing debate has not given a clear link between the structure of ecological communities, their stability, and the persistence of the species constituting these communities[14]. As a potential solution, the structuralist approach[15] and its recent application to ecology have shown to provide a parsimonious theoretical benchmark to understand and predict the persistence of empirical ecological communities in changing environments[14, 16].
The main prediction of the structuralist approach is that the network of biotic interactions among species composing an ecological community determines their opportunities to coexist[17]. Communities with larger coexistence opportunities, which in natural plant-pollinator communities correspond to more cohesive structures of biotic interactions (i.e. nested) [14], are likely more persistent because they can tolerate a larger difference in intrinsic growth rates (i.e., performance) among species. Importantly, species performances are expected to be driven by the environment where they live, providing a phenomenological link with the current environmental conditions [18]. The degree of structural stability of an ecological community can be rigorously assessed by coupling mathematical theory to population models that describe the dynamics of the species based on these two ingredients: species´ performance, and their interactions. However, for many communities such as pollinators, information on such performance is not available. In that case, the structuralist approach is still valid because it allows taking a probabilistic view to ask which communities are more likely to be observed given the fact that environmental conditions can produce changes in species performance in multiple directions, that is, increasing performance for some species but simultaneously decreasing it for others [14, 19, 20, 16]. Hence, it is expected that the larger the range of species performance compatible with its persistence, the larger the environmental fluctuations that the community can withstand., and the more probable its persistence.
Despite this theoretical framework providing a set of clear predictions and associated tools to assess the persistence of ecological communities, direct empirical tests are lim-

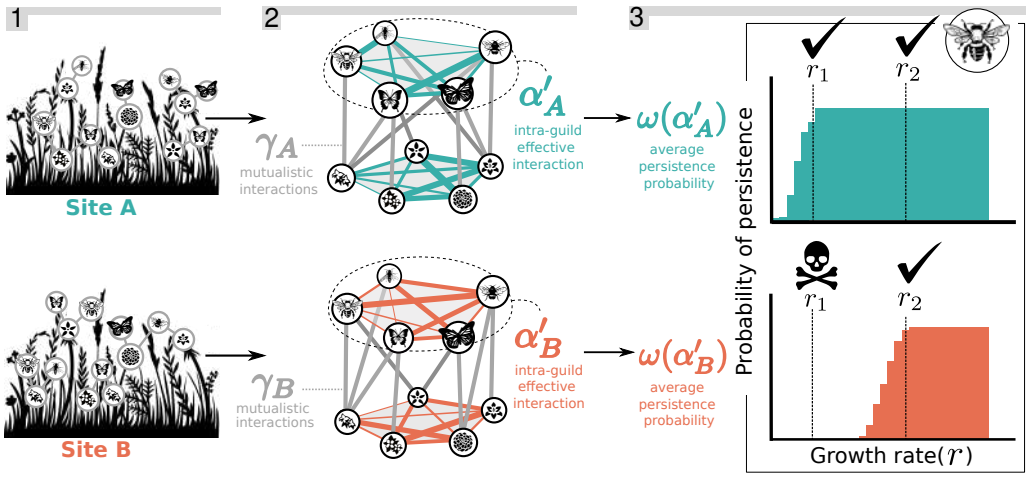

Figure 1: Species' persistence probability in model communities: 1) Empirical observations determine the mutualistic plant-pollinator interactions (γ) of our dynamical model . 2) From γ we obtain a matrix describing the intra-guild effects among pollinators (α'), called "effective interaction matrix" (see Methods). 3) α' is then used to quantify the structural stability (see Methods) , which gives the average probability that any species in the community persists ($\omega(\alpha')$). At the species level, the different distribution of growth rates compatible with a given species persistence (*Anthophora bimaculata* in this example) in sites A and B (colour coded) will determine the likelihood of that species persistence when reproductive rates are sampled randomly ($r1, r2$). Note that fewer values of r are compatible with species persistence in site B (i.e. it has a lower expected persistence probability, ω_i).

ited to micro- [21] or meso-cosmos experiments [22] and real-world tests are still lacking, (but see [16, 23] for an approximation). These tests are of fundamental importance to ensure that the transfer of basic ecological knowledge to conservation planning is relevant in the real world. Part of this lack of progress comes from the difficulty of following plant-pollinator communities over long periods of time [24, 25, 26, 27]which means that most of the empirical plant-pollinator networks studied are just a snapshot of a particular state of the community.

Here, we use a well-resolved data set on abundances and interactions between plants and pollinators in a long-term study carried out on twelve independent sites exposed to changing environmental conditions over 6 years (adding up to 179 pollinator species and 1470 plant-pollinator interactions, see Methods). Following the structuralist approach, we investigated whether empirical observation of species persistence (i.e., the average number of years across sites a species is observed in the community) is explained by the structural stability of the plant-pollinator communities emerging from the species interactions networks. In its probabilistic interpretation, structural stability represents the average probability that a randomly chosen species of the community persists despite varying its performance [18] (see Fig.1). Therefore, we predict that larger values of structural stability promote higher persistence of a pollinator community. To test our main prediction across levels of biological organization (both community- and species-level) we recorded across the 12 independent communities, (i) the abundances of pollinator species over time with which we quantified empirical persistence, and (ii) the mutualistic network of plant-pollinator interactions with which we quantified the structural stability (i.e. the expected average persistence probability, ω). To quantify the average expected persistence of a species in a given community (ω), we need to parameterize a model that describes reasonably well the population dynamics of plants and pollinators in terms of their biotic interactions. For this, we used a standard mutualistic dynamic model [28, 14, 29, 18] where the mutualistic interactions are parameterized with the observed plant-pollinator networks (see Methods and Fig.1). From the plant-pollinator mutualistic interactions, we inferred the matrices describing the effective biotic interactions among pollinators (α'_A), and among plants (α'_P), following previous methodologies (see Methods and SI.H).Taken together, these matrices of species interactions determine the range of species' growth rate values (r) compatible with its persistence[14]. In what follows we center our results on pollinators, but we advance that the framework also works to describe and predict which are the more persistent plant species (see Fig.S1-S2).

Results and discussion

Although our analyses indicate a moderate change in the expected average persistence probability (ω) across all 12 independent sites (ranging from 0.45 to 0.55), we find that this variation was sensitive enough to capture differences in empirical persistence between pollinator communities. Note that we studied natural communities within a single habitat type and for which the main drivers of environ-

mental change are related to its fragmentation degree over space and weather variability over time. Hence, we do not expect large changes in species persistence, in contrast to comparisons across habitats, or in situations where most of the focal habitat has been destroyed[4].

According to our main hypothesis, we observe that those pollinator communities with higher opportunities for species to coexist (i.e., with higher average persistence probability, ω) strongly correspond with higher mean pollinator persistence observed in the field (Spearman correlation coefficient, henceforth called ρ, of 0.85) as shown in Fig.2.A. This result indicates that the structure of species interactions in the studied communities contains information on how can species, on average, persist under changing environments (a result that holds when excluding species only observed once, see Fig.S3).Interestingly, our results additionally suggest that landscape fragmentation matters for determining the observed variation in the expected persistence probability with communities in larger habitat patches tending to exhibit higher persistence (correlation $\rho \approx 0.6$) and a more nested structure ($\rho \approx 0.7$) than those in smaller patches (Fig.S4.B),but not necessarily more diverse in species (Fig.S4.C).Note, however, that most of this trend in nestedness seems to be due to an increase in degree heterogeneity with patch size (Fig.S4.D).Hence, landscape fragmentation, one of the consequences of more intensive agricultural practices, can have a negative impact on the ability of the species to withstand other changes, such as climate change.

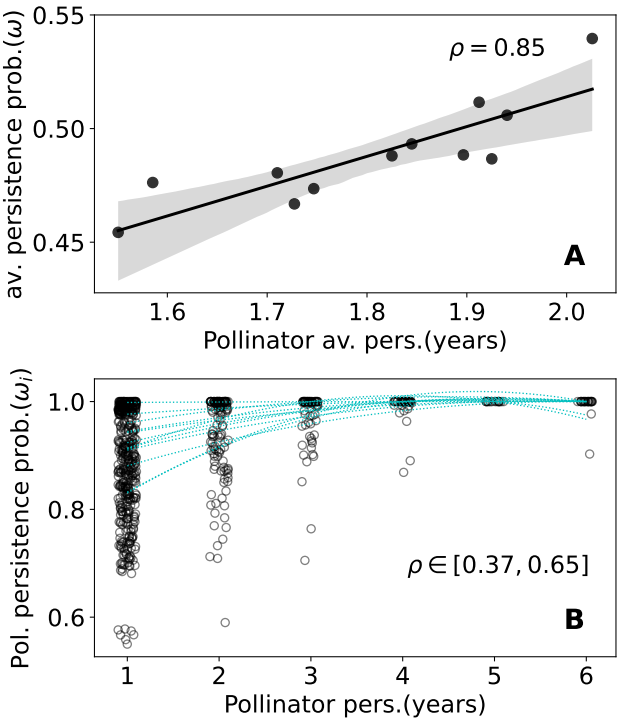

Figure 2: Theoretical expectation vs empirical values. A, Expected average persistence probability of pollinators (ω) versus mean persistence observed in the field for the 12 sites in the study. The shaded area represents the 95% confidence interval of the regression estimate. B, Expected pollinator persistence probability (ω_i) versus the number of years this pollinator is present in the field. Each point represents one pollinator species in one site, and all 12 sites are plotted together but analyzed independently. The dotted blue lines represent the 50 quantile regression for each of the 12 sites, Spearman's rank correlation coefficient (ρ) is shown for the upper figure, and its range depending on the site on the lower figure. Note the differences in the x-axis between panels A and B. While panel A indicates an average persistence in the field between 1.5 and 2 years across species, panel B represents the number of years each pollinator species was observed in the field (from one to six).

While these results can give us information on the whole community, from a conservation point of view is often important to also study the persistence of the individual species, especially those that are rare, endemic, or threatened. For that, we quantified the expected probability of persistence for each species in the 12 studied communities (ω_i)[20, 16], and compared such probabilities with the number of years each species is present in the field (Fig.2.B and Fig.S5).In agreement with our main prediction, we also find a positive relationship between the expected pollinator persistence probability in the model (ω_i) and the number of years that a pollinator is found in the field (ρ ranges from 0.37 to 0.65 depending on the site, and is always statistically significant), meaning that species that are more frequently expected to be locally extinct in the theoretical models also tend to have lower observed persistence in real communities. Some of the species more frequently predicted to be extinct are comparatively rare species (Fig.S6a).Prior work suggests that the link between rare species and their lower probability to persist occurs when species are under a process of extinction debt[30], or, in open systems like our empirical communities, they represent transient species just "passing through", subject to source and sink dynamics[31, 32].

In line with the theoretical developments, our analysis uses information on who interacts with whom (i.e. unweighted mutualistic interaction networks) and a presence-absence metric of persistence. However, species abundances can still be a confounding factor if they drive both the structure of species interaction networks and the probability of species persistence. Using null models that generate randomized species interaction networks only from the species abundance distributions[33] we show that despite we are able to recover a general nested structure in the networks from the null model (Fig.S12),we do not recover who interacts with whom (see also [34] for similar results). Interestingly, the structural stability of these randomized interaction networks does not explain the observed pollinator persistence (Fig.S13), indicating that besides the general correlation between the interaction network structure and

expected persistence [14], who interacts with whom is the key factor for predicting species persistence. In fact, further analyses involving null models shows that the particular degree sequence of the empirical networks is one major driver of their structural stability (Fig.S17). A detailed analysis of the effect of species abundance as a confounding factor can be found in SI I and J, and a detailed comparative with all the null models explored in SI K.

Our results therefore highlight that the structuralist approach is a useful theoretical framework to progress our mechanistic understating of two interrelated problems in ecology: the identification of dynamically stable species that persist despite environmental fluctuations[35], and how such stability permeates from species to communities[10].

Species might persist despite presenting strong temporal fluctuations in their abundances[36]. Thus, a natural next question to ask is whether this framework can not only identify persisting species, but also species with stable temporal fluctuations in abundance. Overall, we found no correlation between our theoretical measure of persistence (expected average persistence probability, ω) and the observed temporal stability of the aggregated pollinator population (S) ($\rho = 0.24$, not statistically significant), suggesting that structural stability is not a good predictor of temporal stability at the community level. If the structuralist approach is not a strong predictor of temporal stability, it opens the field to investigate which are instead its predictors. To shed light on this point, we performed a linear regression accounting for the three main variables known to drive temporal stability in plant and pollinator communities: species richness[37], temporal stability of species' populations[38], and population asynchrony[39] (see Methods). Among these predictors, both pollinator richness (Fig.3.A), and temporal stability of pollinators' populations (Fig.3.B) were weakly and non-significantly correlated with the temporal stability of the community. Instead, more temporally stable communities are composed of pollinators with strong asynchronous responses (Fig.3.C), a result that we recover also with plants (Fig.S2). This negative relationship, which is a common phenomenon observed in empirical studies including pollinators[40], is known as biodiversity insurance or portfolio effect[41], and it indicates that the persistence dynamics that capture the structuralist approach are independent of those captured by the temporal stability of the community. While structural stability informs of the average persistence of communities and species, temporal stability informs of the asynchronous temporal fluctuation. At the species level, however, we found a weak but significant positive correlation between structural and temporal stability, caused by a subset of abundant species that sustain stable populations with a high expected probability of persistence (Fig.S7).

Ecology is entering an exciting phase where models based on solid theory are being used to simultaneously understand ecological processes and predict the fate of ecological communities under global change [7]. Under these circumstances, the resurgence of monitoring programs, including ambitious pollinator ones[42, 43], holds great potential to seek the perfect empirical and theoretical marriage to rigorously describe and predict temporal changes in pollinator populations, which can directly allow to better inform conservation and management decisions. Here we build on prior work that highlights the importance of applying the structuralist approach to the network of biotic interactions to understand the species' demographic consequences [14, 16, 23]. By studying multiple independent sites, we empirically confirm that the interaction network structure of plant-pollinator communities can explain their temporal dynamics across levels of biological organization, a long-lasting open question in ecology [44]. That is, we can distinguish which communities and which particular species are more likely to persist or will die out in the face of ever-present environmental variation, thus providing promising tools for management that might allow designing actions to combat pollinator loss. Taken together, our results show the power to couple detailed empirical data with mathematical theory and associated modeling tools to understand pollination declines, opening new avenues of study and at the same time, reinforcing previous theoretical results.

Methods

Empirical data: Data on species population and interaction strength has been gathered during empirical observations through six consecutive years (2015-2020) along the spring season (from February to June). Each year we sampled twice a month for at least seven rounds during the full flowering season across 12 different sites situated in a landscape fragmentation gradient in the southwest of the Iberian peninsula (Huelva and Seville), gathering data on plant-pollinator interaction frequency and flower abundance. Sites where at least 3 km apart (mean 7,17±0.97 km, Fig.S9) which is larger than the foraging distances of most pollinators [45] and hence can be viewed as independent. In each site, and during each round, we walked a 100 m straight line for 30 minutes in which we wrote down every plant-pollinator interaction seen, differentiating between the number of pollinator individuals, and the number of visits per individual. This resulted in a total of more than 250h of field observations. In addition, we measured the abundance of plants by recording the number of flowers of each plant species in ten $1m^2$ subplots placed along the transect. Bees and plants that we were unable to identify *in situ* were collected for later identification. The time spent collecting specimens was discounted from the standardized sampling time. Bees were caught by hand-netting and preserved

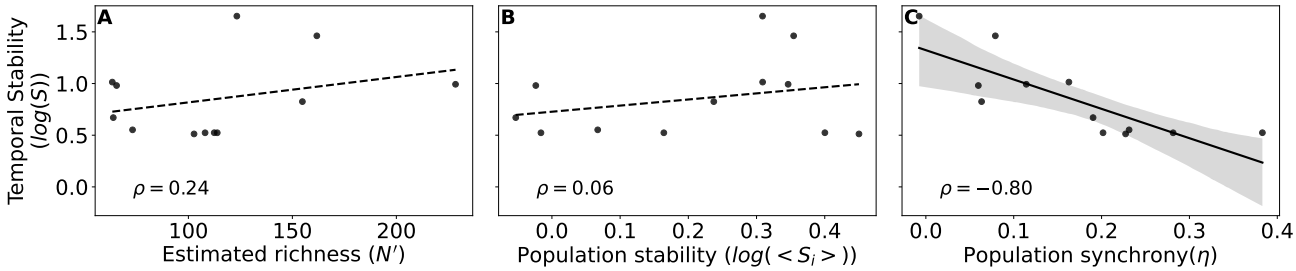

Figure 3: Dependence of temporal stability of the aggregated pollinator population ($log(S)$) on A, pollinator estimated richness (N'), B average pollinator population stability($log(< s_i >)$), and C, synchrony of pollinator populations(η). The shaded area represents the 95% confidence interval of the regression estimate. Each point represents one study site, and each figure includes Spearman's rank correlation coefficient(ρ) and the regression line (dashed when not statistically significant).

in a freezer at -20ºC until they could be pinned and labeled in the lab, and plants were preserved using plant presses. Later F.P.M. identified them using a binocular loupe and determination keys. Those specimens which identification was unclear were sent to taxonomic experts. While non-collected pollinators might be double counted in transects, we believe this is unlikely given the behavior of solitary bees, and in any case, this will not affect our main analysis based on unweighted metrics This intensive fieldwork resulted in a dataset containing more than 179 pollinators and 1470 plant-pollinator interactions (see Table S1).

Empirical measures of persistence and temporal stability: We obtained the yearly floral abundance of plant species in each site by aggregating the abundance of all rounds in the year. We measured pollinators' yearly abundance by aggregating through each year the number of times each pollinator species had interacted with any plant. Note that we recorded both the number of individuals and the number of visits per individual, and abundance metrics were always derived from individual counts, not visitation frequencies, to avoid confounding pollinator activity with its frequency. In both cases, we normalized the abundances with the sampling effort of that year (i.e. the number of rounds).

To quantify the **persistence** of each species in each site, we measured the number of years the species was present in the field, and then obtained the mean persistence of plants and pollinators in each site as the average persistence of the species present in the site.

We quantified **temporal stability** of plant and pollinator populations at two scales. At the community scale, we first obtained the total abundance of pollinators and flowers for each year by aggregating the abundance of all the species in the site, and then we measured the inverse of the coefficient of variation (σ/μ) [37] of such aggregated abundances. At the species scale, we measured for each species in each site the inverse of the coefficient of variation (σ_i/μ_i) of the species abundance through the 6 years. We verified that the relationship between μ and σ was linear (Fig.S14), and hence, our metric is appropriate to measure community stability[46], since temporal stability is not merely driven by mean abundance (see Fig.S15 and SI J).

We quantified **species richness** (N') with the asymptotic species richness estimator, using package iNEXT in R[47], to avoid the possible influence of sampling effort in determining true species richness.

We quantified species average **synchrony** (η) as the mean correlation coefficient between the field abundances A_i of each species i versus the rest of the community (all A_j except i) following[39] as

$$\eta = (1/N) \sum_i r(A_i, \sum_{j \neq i} A_j)$$

and verified that it was not simply a consequence of species' abundances (Fig.S16 in SI J).

Empirical interaction networks: We obtained the network of interactions in each site by aggregating through all the years the identity of the interactions recorded between plants and pollinators. This ensures a proper characterization of all potential interactions realized in our communities since sample coverage (measured also using package iNEXT in R[47]) was above 0.85 in all sites. To build a model as parsimonious as possible we only used unweighted interactions in the mutualistic model (i.e. $M_{ij} = 1$ if species i and j interacted in the field and 0 otherwise) as is usually done in this type of models[14, 29, 18].

The mutualistic model: To quantify the average persistence probability (ω) we employed a standard mutualistic dynamics model[28, 14, 29, 18], using the empirical networks as the skeleton (see below). The equations describing the abundance of plants (P_i) and animal (A_i) species are of the form:

$$\begin{bmatrix} \frac{dP}{dt} \\ \frac{dA}{dt} \end{bmatrix} = diag\left(\begin{bmatrix} P \\ A \end{bmatrix}\right) \times \left(\begin{bmatrix} r_P \\ r_A \end{bmatrix} - \underbrace{\begin{bmatrix} \alpha_P & -\gamma_P \\ -\gamma_A & \alpha_A \end{bmatrix}}_{\mathbf{A}} \begin{bmatrix} P \\ A \end{bmatrix} \right) \quad (1)$$

with parameters accounting for intrinsic growth rate (r), intraguild competition (α) and mutualistic benefit (γ). We considered mean field intra-guild competition ($\alpha_{ii}^P = \alpha_{ii}^A = 1$, $\alpha_{ij}^P = \alpha_{ij}^A = \alpha$), and used the empirical networks to parametrize the mutualistic benefit as follows: $\gamma_{ij} = (\gamma_0 M_{ij})/(k_i^\delta)$, where $M_{ij} = 1$ if we recorded a plant-pollinator interaction between species i and j in the field and zero otherwise, γ_0 represents the overall level of mutualistic strength, and δ the mutualistic trade-off. The results in the main text correspond to α=0.005, γ_0=0.1, and δ=0, but we checked the robustness of the results in SI.L using values of γ_0 below the critical threshold to ensure that all our simulated communities were linearly stable[29]. While improvements can be made (e.g. considering non-linear functional responses [48] or empirically based competition instead of mean field [49]), we chose this model for simplicity and because it is used in many previous theoretical studies.

In order to treat pollinators and plants separately, we worked in an **effective interaction framework**[14], where the mean-field competition between plants and animals is modified by the mutualistic interactions. Diagonalizing the interaction matrix (**A** in equation 1 and 2) per block allows going from a set of $N_P + N_A$ entangled equations for the abundances of plants and pollinators in the steady state (eq.2), to two sets of equations, one for plants (N_P species) and one for pollinators (N_A species), with only intra-guild interactions (eq.3). This is achieved by multiplying by the matrix $T = 1 + \Gamma C^{-1}$ both left sides of equation 2 (see SI H for a more detailed explanation):

$$\begin{bmatrix} r_P \\ r_A \end{bmatrix} = \left(\overbrace{\underbrace{\begin{bmatrix} \alpha^P & 0 \\ 0 & \alpha_A \end{bmatrix}}_{\mathbf{C}} - \underbrace{\begin{bmatrix} 0 & \gamma_P \\ \gamma_A & 0 \end{bmatrix}}_{\mathbf{\Gamma}}}^{\mathbf{A}} \right) \begin{bmatrix} P \\ A \end{bmatrix} \quad (2)$$

$$\begin{bmatrix} r'_P \\ r'_A \end{bmatrix} = \begin{bmatrix} \alpha'_P & 0 \\ 0 & \alpha'_A \end{bmatrix} \begin{bmatrix} P \\ A \end{bmatrix} \quad (3)$$

We quantified the expected average persistence probability (ω) using matrices α'_A and α'_P in equation 3 with the code provided in a previous study[29].

To calculate the persistence probability of a particular species in the model community (ω_i), we used the **structural forecasting framework**[20, 16]. We randomly sampled 3000 directions of r-vectors uniformly inside the full parameter space and solved the systems of equations 3 to determine the proportion of cases in which each species was present in the community($P_i, A_i > 0$).

Nestedness analysis: We quantified the nestedness of the empirical plant-pollinator networks using two metrics: ν, following [29], and $\bar{\nu}$, following [50]. This last metric is a measure of how nested is a given interaction network once the expected nestedness given its degree sequence has been discounted (i.e. if the network is more or less nested than what could be expected given the degrees of the species in the network). In this metric values close to 1 indicate no significant nestedness, while larger values indicate increasing significant nestedness). See SI C for more details.

Disentangling the effect of abundance in determining interaction structure: We tested to what extent the abundance of species could be acting as a potential confounding factor, explaining the results obtained. We implemented the null model presented by Vazquez et al. [33] (named "A"), which generates interaction networks such that the species-specific probabilities of interaction are proportional to species' abundances. We generated 100 randomized versions of each of the empirical interaction networks using the *vaz_null_external* function of package Bipartite in R[51], introducing the empirical species relative abundances as input, and compared both the cumulative degree distribution (Fig.S11) and the expected persistent probabilities (Fig.S13) of the randomized networks with those obtained for the empirical networks. See SI I for more details.

Structural features driving structural stability: To assess the importance of network structure in determining structural stability, we compared measurements of that feature on empirical networks with measurements performed on 100 randomized versions of those networks keeping some properties fixed. Apart from the null model already presented (null model "A"), we used other three different null-models, which – going from the least to the most constraining – are as follows: "B" keeps constant the number of species in each species set and the number of interactions, "C" adds the constraint of keeping also the degree distribution, and finally "D" keeps the degree of each node constant but reshuffle the interactions. The expected pollinator average persistence probability (ω) of empirical networks compared with that measured in their randomized counterparts can be seen in Fig.S17. See SI K for more details.

Correlations and regression estimates: Regression estimates from Fig.2 and 3 were obtained using package seaborn in Python. All Spearman's rank correlation coefficients were obtained using package scipy in Python. The quantile regressions of Fig.2 were obtained using package statsmodels in Python.

Data availability: Dataset of species interaction and abundances can be accessed via Zenodo [52].

Code availability: The code used in this study can be downloaded from Zenodo [52].

Acknowledgments We thank taxonomists Luis Oscar Aguado and Thomas Wood. This project has received funding from the European Union's Horizon 2021 research and innovation programme under the Marie Skłodowska-Curie grant agreement No 101064340 to V.D.-G. This research was funded through the 2017-2018 Belmont Forum and BiodivERsA joint call for research proposals, under the BiodivScen ERA-Net COFUND programme, and with the funding organisations AEI, NWO, ECCyT and NSF to I.B and V.D.-G, TASTE Project (PID2021-127607OB-I00) to O.G, I.B., and V.D.-G, and BeeFUN project (PCIG 14-GA-2013-631653) to IB.

Author contributions V.D.-G., O.G. and I.B. designed research; F.P.M and I.B. did field work and F.P.M identified species; V.D.-G. developed code and analyzed data; V.D.-G. and I.B. performed research; V.D.-G., O.G. and I.B wrote the paper.

Competing interests The authors declare no competing interests.

References

[1] Ollerton, J., Winfree, R. & Tarrant, S. How many flowering plants are pollinated by animals? *Oikos* **120**, 321–326 (2011).

[2] Potts, S. G. *et al.* Safeguarding pollinators and their values to human well-being. *Nature* **540**, 220–229 (2016).

[3] Potts, S. G. *et al.* Global pollinator declines: trends, impacts and drivers. *Trends in Ecology & Evolution* **25**, 345–353 (2010).

[4] Winfree, R., Bartomeus, I. & Cariveau, D. P. Native pollinators in anthropogenic habitats. *Annu. Rev. Ecol. Evol. Syst.* **42**, 1–22 (2011).

[5] Dicks, L. V. *et al.* A global-scale expert assessment of drivers and risks associated with pollinator decline. *Nat Ecol Evol* **5**, 1453–1461 (2021).

[6] IPBES. (policy report) the methodological assessment report on scenarios and models of biodiversity and ecosystem services (2016).

[7] Dietze, M. & Lynch, H. Forecasting a bright future for ecology. *Front Ecol Environ* **17**, 3–3 (2019).

[8] Grimm, V., Schmidt, E. & Wissel, C. On the application of stability concepts in ecology. *Ecological Modelling* **63**, 143 – 161 (1992).

[9] Ives, A. R. & Carpenter, S. R. Stability and diversity of ecosystems. *Science* **317**, 58–62 (2007).

[10] Domínguez-García, V. *et al.* Advancing our understanding of ecological stability. *Ecology Letters* **22**, 1349–1356 (2019).

[11] Donohue, I. *et al.* On the dimensionality of ecological stability. *Ecology Letters* **16**, 421–429 (2013).

[12] Meerbeek, K. V., Jucker, T. & Svenning, J.-C. Unifying the concepts of stability and resilience in ecology. *Journal of Ecology* **109**, 3114–3132 (2021).

[13] Domínguez-García, V., Dakos, V. & Kéfi, S. Unveiling dimensions of stability in complex ecological networks. *Proceedings of the National Academy of Sciences* **116**, 25714–25720 (2019).

[14] Rohr, R. P., Saavedra, S. & Bascompte, J. On the structural stability of mutualistic systems. *Science* **345**, 1253497–1253497 (2014).

[15] Solé, R. V. & Valls, J. On structural stability and chaos in biological systems. *Journal of Theoretical Biology* **155**, 87–102 (1992).

[16] Medeiros, L. P., Boege, K., del Val, E., Zaldívar-Riverón, A. & Saavedra, S. Observed ecological communities are formed by species combinations that are among the most likely to persist under changing environments. *The American Naturalist* **197**, E17–E29 (2021).

[17] Godoy, O., Bartomeus, I., Rohr, R. P. & Saavedra, S. Towards the integration of niche and network theories. *Trends in Ecology & Evolution* **33**, 287–300 (2018).

[18] Song, C., Rohr, R. P. & Saavedra, S. A guideline to study the feasibility domain of multi-trophic and changing ecological communities. *Journal of Theoretical Biology* **450**, 30–36 (2018).

[19] Song, C., Rohr, R. P. & Saavedra, S. Why are some plant-pollinator networks more nested than others? *J Anim Ecol* **86**, 1417–1424 (2017).

[20] Saavedra, S., Medeiros, L. P. & AlAdwani, M. Structural forecasting of species persistence under changing environments. *Ecol. Lett.* **23**, 1511–1521 (2020).

[21] Tabi, A., Petchey, O. L. & Pennekamp, F. Warming reduces the effects of enrichment on stability and functioning across levels of organisation in an aquatic microbial ecosystem. *Ecol Lett* **22**, 1061–1071 (2019).

[22] Bartomeus, I., Saavedra, S., Rohr, R. P. & Godoy, O. Experimental evidence of the importance of multitrophic structure for species persistence. *Proceedings of the National Academy of Sciences* **118**, e2023872118 (2021).

[23] Allen-Perkins, A., García-Callejas, D., Bartomeus, I. & Godoy, O. Structural asymmetry in biotic interactions as a tool to understand and predict ecological persistence. *Ecology Letters* (2023).

[24] Chacoff, N. P. *et al.* Evaluating sampling completeness in a desert plant-pollinator network. *Journal of Animal Ecology* **81**, 190–200 (2011).

[25] Ponisio, L. C., Gaiarsa, M. P. & Kremen, C. Opportunistic attachment assembles plant–pollinator networks. *Ecol. Lett* **20**, 1261–1272 (2017).

[26] Peralta, G. *et al.* Trait matching and phenological overlap increase the spatio-temporal stability and functionality of plant–pollinator interactions. *Ecology Letters* **23**, 1107–1116 (2020).

[27] Gaiarsa, M. P., Kremen, C. & Ponisio, L. C. Pollinator interaction flexibility across scales affects patch colonization and occupancy. *Nat Ecol Evol* **5**, 787–793 (2021).

[28] Bastolla, U. *et al.* The architecture of mutualistic networks minimizes competition and increases biodiversity. *Nature* **458**, 1018–1020 (2009).

[29] Saavedra, S., Rohr, R. P., Olesen, J. M. & Bascompte, J. Nested species interactions promote feasibility over stability during the assembly of a pollinator community. *Ecology and Evolution* **6**, 997–1007 (2016).

[30] Blanchard, G. & Munoz, F. Revisiting extinction debt through the lens of multitrophic networks and meta-ecosystems. *Oikos* (2022).

[31] Gravel, D., Guichard, F., Loreau, M. & Mouquet, N. Source and sink dynamics in meta-ecosystems. *Ecology* **91**, 2172–2184 (2010).

[32] García-Callejas, D., Bartomeus, I. & Godoy, O. The spatial configuration of biotic interactions shapes coexistence-area relationships in an annual plant community. *Nat Commun* **12** (2021).

[33] Vázquez, D. P. *et al.* Species abundance and asymmetric interaction strength in ecological networks. *Oikos* **116**, 1120–1127 (2007).

[34] Olito, C. & Fox, J. W. Species traits and abundances predict metrics of plant-pollinator network structure, but not pairwise interactions. *Oikos* **124**, 428–436 (2014).

[35] Taylor, S. J. S., Evans, B. S., White, E. P. & Hurlbert, A. H. The prevalence and impact of transient species in ecological communities. *Ecology* **99**, 1825–1835 (2018).

[36] Clark, T. & Luis, A. D. Nonlinear population dynamics are ubiquitous in animals. *Nature ecology & evolution* **4**, 75–81 (2020).

[37] Tilman, D., Reich, P. B. & Knops, J. M. H. Biodiversity and ecosystem stability in a decade-long grassland experiment. *Nature* **441**, 629–632 (2006).

[38] Tilman, D. Biodiversity: Population versus ecosystem stability. *Ecology* **77**, 350–363 (1995).

[39] Gross, K. *et al.* Species richness and the temporal stability of biomass production: A new analysis of recent biodiversity experiments. *The American Naturalist* **183**, 1–12 (2014).

[40] Lázaro, A., Gómez-Martínez, C., González-Estévez, M. A. & Hidalgo, M. Portfolio effect and asynchrony as drivers of stability in plant-pollinator communities along a gradient of landscape heterogeneity. *Ecography* **2022** (2022).

[41] Yachi, S. & Loreau, M. Biodiversity and ecosystem productivity in a fluctuating environment: The insurance hypothesis. *Proc. Natl. Acad. Sci. U.S.A.* **96**, 1463–1468 (1999).

[42] Commission, E. *et al. Proposal for an EU pollinator monitoring scheme* (Publications Office, 2021).

[43] Woodard, S. H. *et al.* Towards a u.s. national program for monitoring native bees. *Biological Conservation* **252**, 108821 (2020).

[44] Bascompte, J., Jordano, P., Melian, C. J. & Olesen, J. M. The nested assembly of plant-animal mutualistic networks. *Proceedings of the National Academy of Sciences* **100**, 9383–9387 (2003).

[45] Kendall, L. K. *et al.* The potential and realized foraging movements of bees are differentially determined by body size and sociality. *Ecology* **103** (2022).

[46] Reckling, M. *et al.* Methods of yield stability analysis in long-term field experiments. a review. *Agron. Sustain. Dev.* **41** (2021).

[47] Hsieh, T. C., Ma, K. H. & Chao, A. iNEXT: an r package for rarefaction and extrapolation of species diversity (hill numbers). *Methods Ecol Evol* **7**, 1451–1456 (2016).

[48] Cenci, S. & Saavedra, S. Structural stability of nonlinear population dynamics. *Physical Review E* **97** (2018).

[49] García-Callejas, D. *et al.* Non-random interactions within and across guilds shape the potential to coexist in multi-trophic ecological communities. *Ecology Letters* **26**, 831–842 (2023).

[50] Jonhson, S., Domínguez-García, V. & Muñoz, M. A. Factors determining nestedness in complex networks. *PLoS ONE* **8**, e74025 (2013).

[51] Dormann, C. F., Gruber, B. & Fruend, J. Introducing the bipartite package: Analysing ecological networks. *R News* **8**, 8–11 (2008).

[52] Domínguez-García, V., Molina, F. P., Godoy, O. & Bartomeus, I. Data and code corresponding to the article 'Interaction network structure explains species temporal persistence in empirical plant-pollinator communities'. *Zenodo* (2023). URL https://doi.org/10.5281/zenodo.10083504.

Contents

Supporting information text

1 Results for plant species

While in the main text we only show results for pollinators, we find that the results for plant species are similar, as shown below.

1.1 Expected persistence probabilities

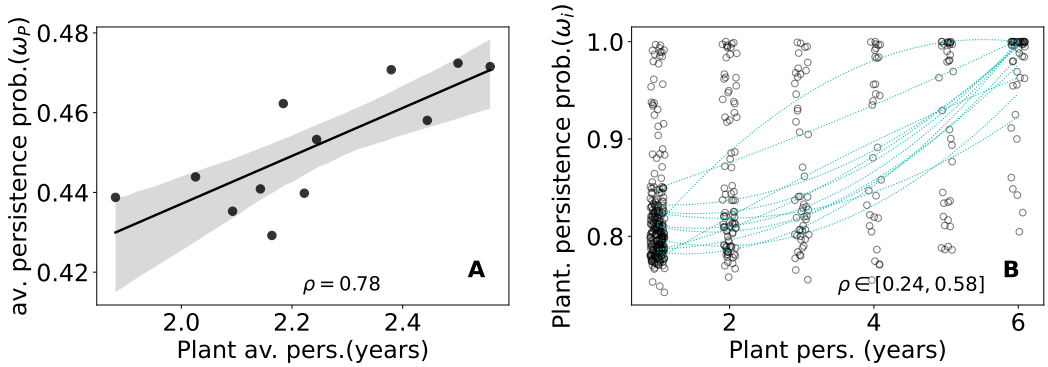

Figure S1: A), Expected average persistence probability of plants (ω_P) versus plant mean persistence observed in the field for the 12 sites in the study. The shaded area represents the 95% confidence interval of the regression estimate. B), Expected plant persistence probability (ω_i) versus the number of years the plant is present in the field. Each point represents one plant species in one site, and all sites are plotted together but analyzed independently. The dotted blue lines represent the 50 quantile regression for each of the 12 sites. Left figure includes Spearman's rank coefficient (ρ), while right figure includes the range of ρ values depending on the site.

1.2 Temporal stability of plant abundance

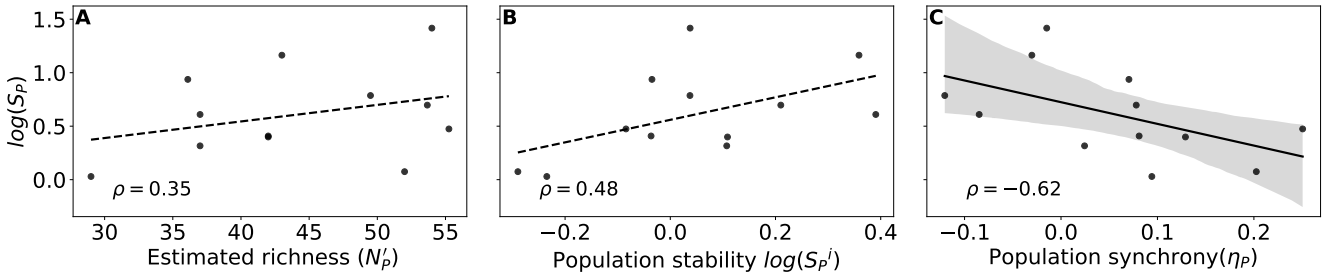

Figure S2: Dependence of temporal stability of the aggregated plant population($log(S_P)$) on A, estimated plant species richness (N_P'), B average plant population stability ($log(< S_P^i >)$), and C, synchrony of plant populations(η_P). The shaded area represents the 95% confidence interval of the regression estimate. Each point represents one study site, and each figure includes Spearman's rank correlation coefficient(ρ) and the regression line (dashed when not statistically significant).

2 Ignoring singleton species

In order to study how much of the correlation between the predicted average persistence probability (ω) and the empirical persistence that we exposed in the main text was driven by rare species we decided to check this relationship when rare pollinator species are not considered (Fig. S3). To do that, we first ignored the pollinator species that only appear once in our study by removing them from the empirical measures of mean persistence and from the model to quantify persistence probability (Fig. S3.B). We also decided to go further and ignore species that have been only recorded at most once during each year, by removing them both from the empirical observations when measuring mean pollinator persistence, and from the model used to quantify persistence probability (Fig.S3.C). While removing singleton species reduces the correlation between mean pollinator persistence in the field and predicted average persistence probability, the correlation remains relatively high and significant in all scenarios.

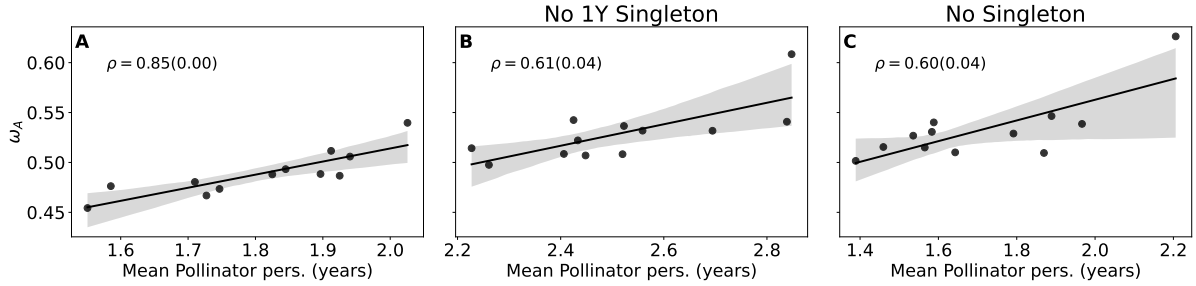

Figure S3: Predicted average persistence probability (ω) vs mean pollinator persistence in the field when A) all pollinator species are considered (as in main text), B) when pollinators that only appear once in the data-set are ignored, and C) when pollinators that only appear once per year are ignored. Each figure includes Spearman rank correlation coefficient(ρ) and the p-value of the two-sided test, to see that they remain significant. The shaded areas represent the 95% confidence interval of the regression estimates.

3 Patch size affects structural stability

The patch size, measured as the area of the focal habitat patch where the transect was located, is positively correlated with the expected average persistence probability of the pollinator communities (ω)(Fig.S4A). This means that landscape fragmentation, one of the consequences of more intensive agricultural practices, can have a negative impact on the ability of the species to withstand other global change drivers, such as climate change. We also observe that communities in larger patches tend to have a more cohesive (i.e. nested[1]) structure of mutualistic interactions (Fig.S4 B). We checked that this nested pattern was not driven by larger patches harboring more species-rich communities (Fig. S4C). When we quantified nestedness using a different metric that takes into consideration the degree heterogeneity of the network ($\tilde{\nu}$) [2] instead of just quantifying the number of shared partners (ν) [1], all the networks were more nested than what could be expected given their degree sequence (Fig. S4D, note that values of nestedness in the figure are above 1). However, we do not see a relationship between this nestedness metric ($\bar{\nu}$) and patch size, which hints to an increase in degree heterogeneity (i.e. more specialists, and more generalist species) with patch size that is not caused by species richness (note that ν is mainly determined by the degree heterogeneity [2]).

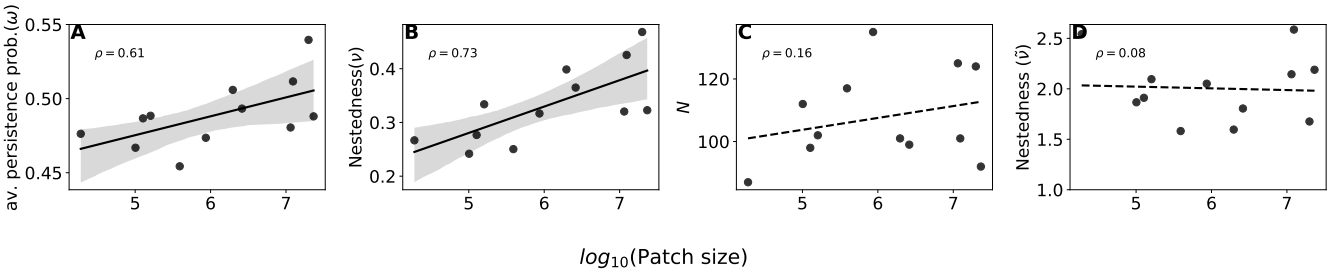

Figure S4: A, Predicted average persistence (ω) vs Patch size. B, Nestedness (ν) of the mutualistic interaction network vs Patch size. C, Species richness of the mutualistic networks vs patch size. D, Nestedness measure controlling for degree sequence ($\bar{\nu}$) vs patch size. All figures include the Spearman's rank correlation (ρ), and a regression line (dashed when not significant). The shaded areas represent the 95% confidence interval of the regression estimates.

4 Persistent probability vs empirical persistence site by site

While in the main text we plot all sites together for showing the result of how the correlation between the persistent probability given by the model (ω_i) correlates with the empirical persistence in the field (Fig. 2B), here we show this positive correlation for each site independently (Fig.S5).

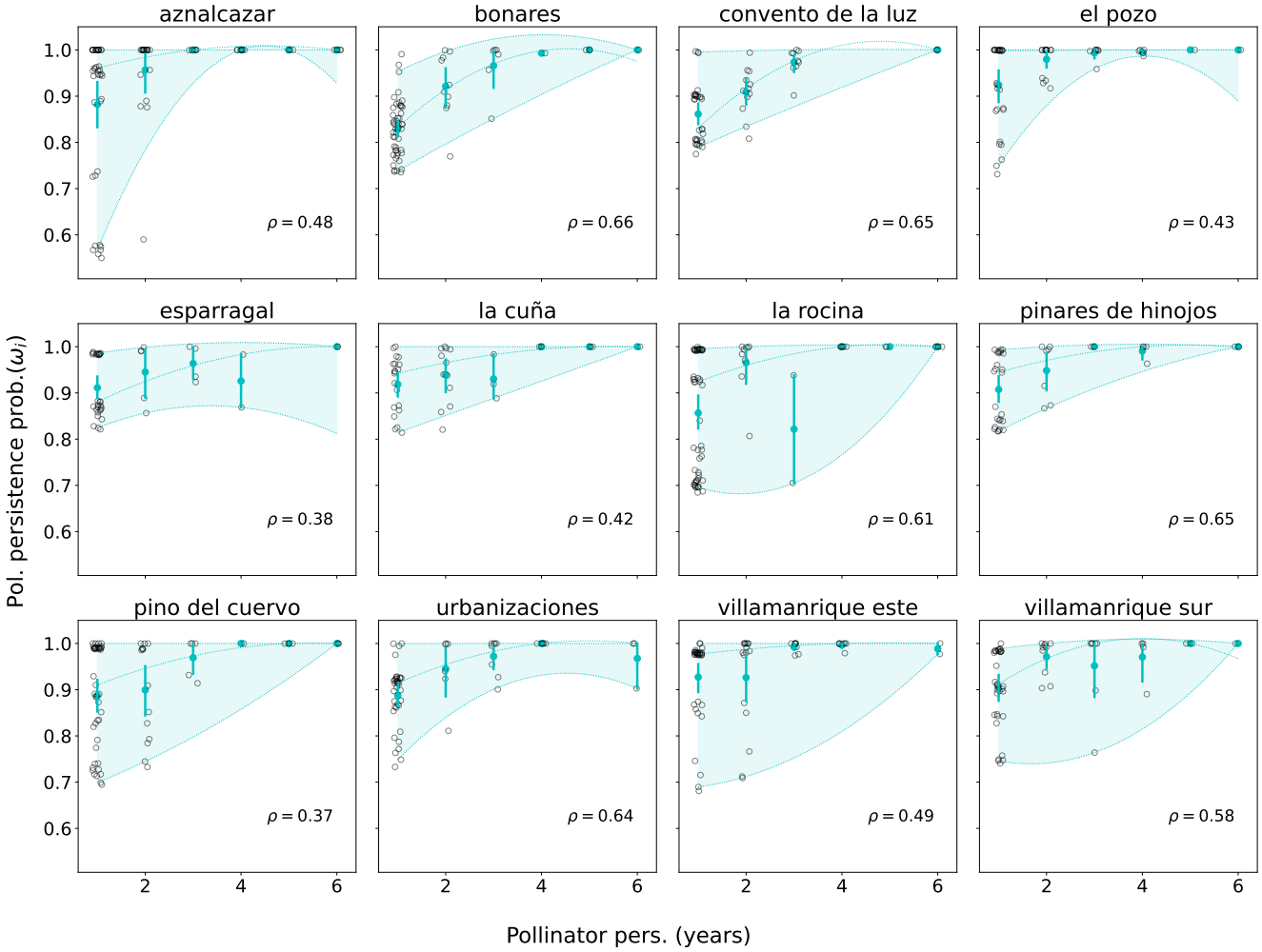

Figure S5: Predicted pollinator persistence probability (ω_i) versus the number of years the pollinator is present in the field. Each point represents one pollinator species in one site, and each panel represents one study site. The shaded regions represent the 5-95 quantile regression. The round points indicate the mean value of ω_i for pollinator species that persist from 1 to 6 years, and the error bars one standard deviation. All figures include Spearman's rank correlation coefficient (ρ).

5 Species' persistence probability and abundance

Comparing species abundance in the field (quantified as the % of abundance each species represents in the community) with its expected persistence probability in the model (ω_i), shows that species with lower predicted persistence probabilities are always the least abundant. Said otherwise, it is evident that more abundant species are always predicted to survive in the model communities (Fig.S6a). As can be seen in Fig.S6a, while there is not a univocal relationship between the expected pollinator persistence and their field abundance, there is a clear positive relationship between them ($\rho \in [0.32, 0.72]$,which is significant in all sites), and similarly can be said about plants.
Comparing species abundance in the field with their persistence in the field shows a similar but stronger trend, where more abundant species are always present, but the least abundant species can be highly persistent (being present 5 or 6 years) or not persistent at all (being only 1 or 2 years) (Fig.S6b).Note that while a correlation exists, abundance can not fully explain species persistence.

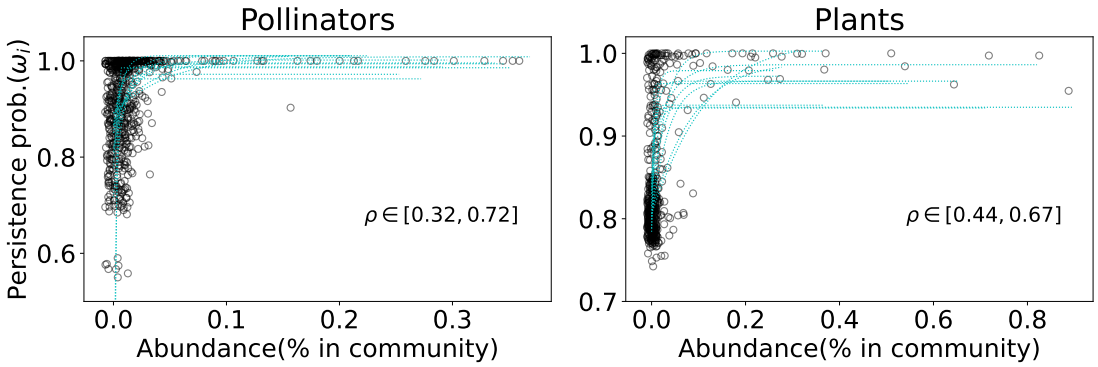

(a) Species' probability of survival in the model (ω_i) vs. its abundance in the field for pollinators (left) and plants (right). Each figure includes the range of values of the Spearman's rank correlation coefficient (ρ) depending on the site. The dotted lines are the best fit for each of the 12 sites in the study.

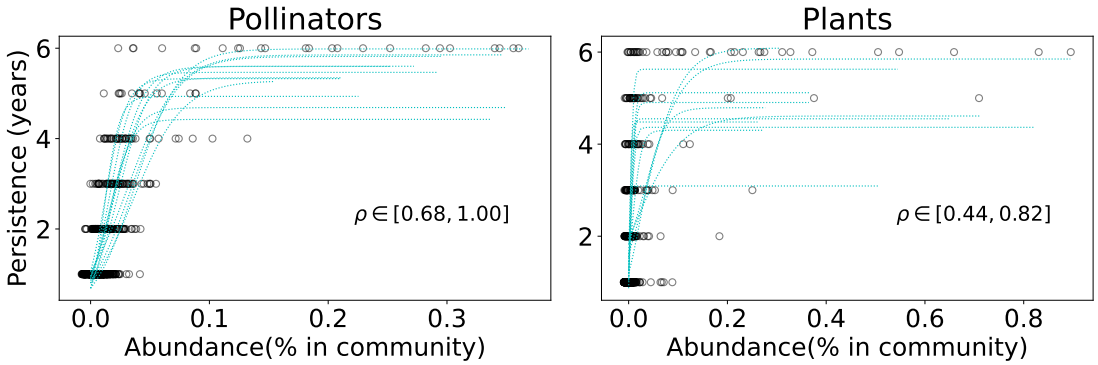

(b) Species' persistence in the field vs. its abundance in the field for pollinators (left) and plants (right). Each figure includes the range of values of the Spearman's rank correlation coefficient (ρ) depending on the site. The dotted lines are the best fit for each of the 12 sites in the study.

Figure S6

6 Species' temporal stability, expected persistence probability and persistence

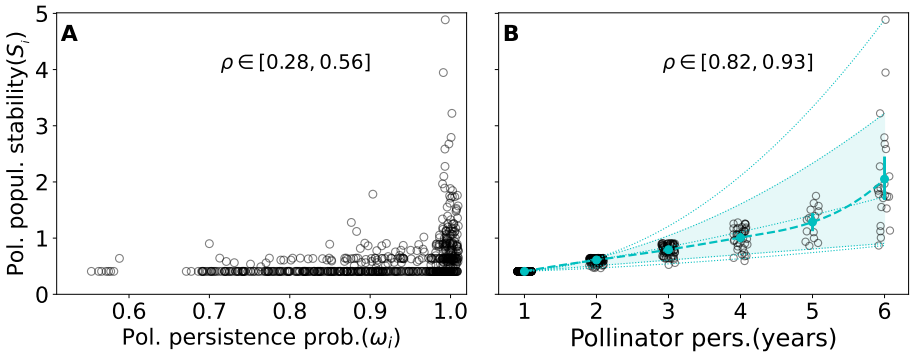

Figure S7: Observed temporal stability of pollinator abundances (S_i) versus A, pollinator persistence probability predicted by the mutualistic model (ω_i), and B, the number of years the pollinator is present in the field. The round points indicate the mean value of S_i for pollinator species that persist from 1 to 6 years in the field, with the errorbars representing one standard deviation, and the dashed line is a help to the eye. Shadow areas represent the 5-95 quantile, and the area inside the blue line is the 1-99 quantile. Both figures include the ranges of Spearman rank correlation coefficients (ρ) in the different study sites.

While at the community level we found no significant correlation between the predicted average persistence probability (ω) and the temporal stability of the aggregated pollinator population (S), at the species's scale we found a weak but significant positive correlation between pollinator's expect3ed persistence probabilities (ω_i) and its population temporal stability(S_i) ($\rho \in [0.28, 0.56]$, significant in all sites but one) Fig.S7.A). This correlation coefficient could suggest that pollinators predicted to persist tend to present more stable populations, but the spread on the y-axis values for pollinators with high persistence probability shows that these pollinators do not necessarily present stable populations. Pollinators with more stable populations are always predicted to survive, but not all pollinators predicted to survive necessarily sustain stable populations in time. Indeed, looking at the temporal stability of population populations (S_i) vs their persistence in the field (Fig.S7.B) also shows that more persistent pollinators exhibit larger variations in their population stability ($\rho \in [0.82, 0.93]$, significant in all sites but one). As for the strong positive correlation in the figure, the result is not too surprising given how temporal stability is defined, yet it clearly indicates that pollinators with lower observed persistence (i.e., those that are observed fewer number of years in the community) tend to have more variable populations, while pollinators that are repeatedly observed in the community one year after another, show larger variation in their population stability, but overall present more stable population over time. Again, we find a similar result for plants (Fig.S8).

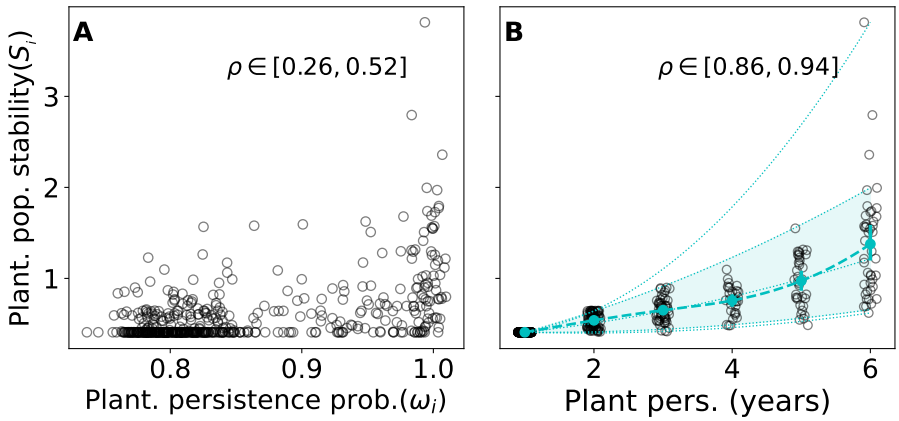

Figure S8: Observed temporal stability of plant abundances (S_i) versus A, plant persistence probability predicted by the mutualistic model (ω_i), and B, number of years the plant is present in the field. The round points with error bars indicate the mean value of S_i for plant species that persist from1 to 6 years, with one standard deviation, and the dotted line is just a help to the eye. Shadow areas represent the 5-95 quantile, and the area inside the blue line the 1-99 quantile. Both figures include the ranges of Spearman rank correlation coefficients (ρ) in the different study sites.

Supporting information for Methods

7 Dataset

Site	Area (m^2)	Plant sp.	Pollinator sp.	nº interacciones
pinares de hinojos	23220000	24	40	81
aznalcazar	19900000	24	78	178
el pozo	12380000	25	57	121
pino del cuervo	11500000	26	69	139
villamanrique sur	2610000	19	58	114
villamanrique este	1970000	20	67	131
la rocina	865000	27	75	147
bonares	390000	23	69	132
urbanizaciones	160000	24	58	143
la cuña	127000	22	40	88
convento de la luz	101000	25	55	123
esparragal	19000	21	41	73

Table S1: Summary statistics of the interaction networks in our study. From left to rights columns indicate the name of the site, its area, the number of different plant species recorded, the number of pollinator species recorded, and the number of interactions recorded (not the frequency).

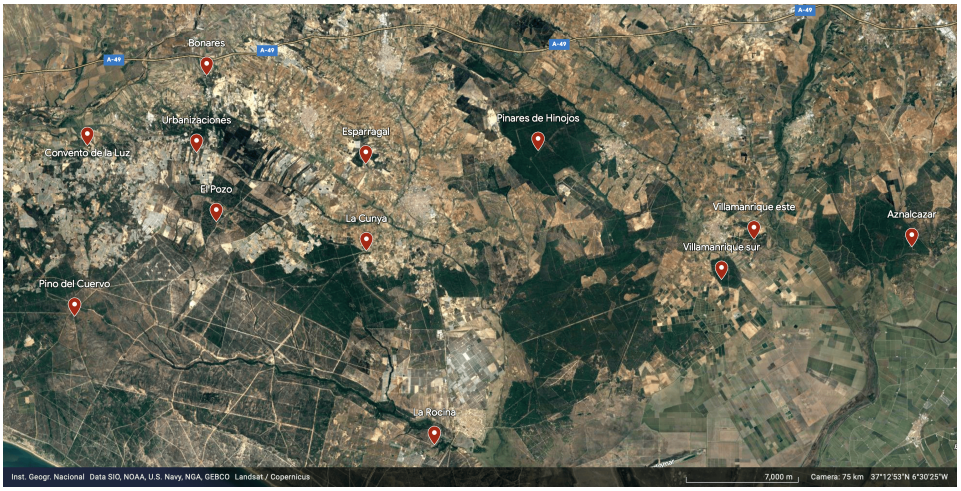

Figure S9: Map of the 12 sites studied along a fragmentation gradient. Reproduced from Google Earth Pro 7.3.6.9345.(December 29, 2022). Doñana Region, SW Spain. 37° 12' 53"N, 6° 30' 25"W, Eye alt 7000 m. Borders and labels; places layers. Inst. Geogr. Nacional, SIO, NOAA, U.S. Navy, NGA, GEBCO. Landsat/Copernicus. http://www.google.com/earth/index.html (Accessed August 2, 2023)

8 Deriving effective biotic interaction matrices

In order to disentangle plant and pollinator systems we apply the transformation presented in [3], multiplying both left sides of equation 1 by $T = 1 + \Gamma C^{-1}$. The transformations allow going from this system where plants and pollinators are entangled ($N_P + N_A$ equations)

$$\begin{bmatrix} r^P \\ r^A \end{bmatrix} = \left(\overbrace{\underbrace{\begin{bmatrix} \alpha^P & 0 \\ 0 & \alpha^A \end{bmatrix}}_{\mathbf{C}} - \underbrace{\begin{bmatrix} 0 & \gamma^P \\ \gamma^A & 0 \end{bmatrix}}_{\mathbf{\Gamma}}}^{\mathbf{A}} \right) \begin{bmatrix} P \\ A \end{bmatrix} = -\hat{A} \begin{bmatrix} P \\ A \end{bmatrix} \tag{1}$$

to these two disentangled systems, one for plants (with N_P equations) and another for pollinators (with N_A equations)

$$\begin{bmatrix} r^P + \gamma^P (\alpha^A)^{-1} r^A \\ r^A + \gamma^A (\alpha^P)^{-1} r^P \end{bmatrix} = \begin{bmatrix} \alpha^P - \gamma^P (\alpha^A)^{-1} \gamma^A & 0 \\ 0 & \alpha^A - \gamma^A (\alpha^P)^{-1} \gamma^P \end{bmatrix} \begin{bmatrix} P \\ A \end{bmatrix} \tag{2}$$

that represents the effective intra-guild interaction once the competition and mutualistic effects have been taken into account

$$\begin{bmatrix} r'_P \\ r'_A \end{bmatrix} = \begin{bmatrix} \alpha'_P & 0 \\ 0 & \alpha'_A \end{bmatrix} \begin{bmatrix} P \\ A \end{bmatrix} \tag{3}$$

In this new framework r'_P and r'_A are called effective intrinsic growth rates and α'_A and α'_P effective interaction. These two matrices are the ones we use to quantify the structural stability of the pollinator community and of the plant community.

8.1 Reconstructing persistence probability of the full plant-pollinator communities

Since we are working with the effective interaction matrices instead of the original representation, we studied to what extent the expected persistence probability of the effective interaction systems was representative of the original community with mutualism and mean field competition. Here we show that we can recover almost perfectly (up to 97%) the persistence probability of the whole community (ω_C) as a combination of the persistence probability of plants and pollinators (ω_P and ω_A).

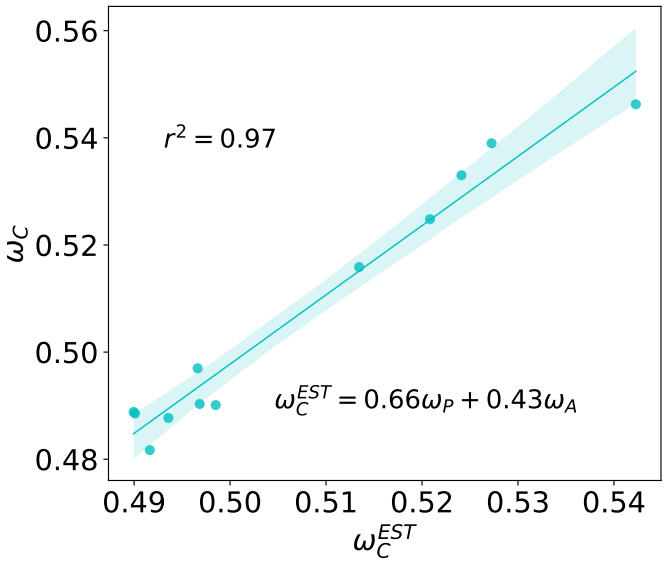

Figure S10: Average persistence probability of the full plant-pollinator mutualistic communities (ω_C) vs the estimated average persistence probability of the plant-pollinator community (ω_C^{EST}). The text shows the best estimation for average persistence probability (ω_C^{EST}) as a combination of the average persistence probability of the effective biotic matrix interaction of plants (ω_P) and pollinators (ω_A), as well as the goodness of the reconstruction (r^2). The shaded area represents the 95% confidence interval of the regression estimate.

9 Role of abundance in determining interaction structure

We tested to what extent the abundance of species could be driving both the species interaction networks and species persistence (see below in this section), and act as a potential confounding factor explaining the results obtained. We did that by implementing the null model presented by Vazquez et al.[4] (named null model "A"), which generates interaction networks based on species abundances, and comparing the generated random interaction networks with the empirical ones in our study. The mentioned null model randomizes the total number of individual interactions observed in the original interaction matrix, F, so that the species-specific probabilities of interaction are proportional to the species' relative abundances. We generated 100 randomized versions of each of the empirical interaction matrices using the *vaz_null_external* function of the package *bipartite*, and compared the cumulative degree distribution of our empirical networks with their randomized counterparts. As can be seen in Fig.S11 the degree distributions of the networks generated by the null model (in blue) are really different from the empirical ones (in red). In particular, we find that the null model greatly underestimates the specialist species (note that the minimum degree is two in all networks) and the hubs have a much higher degree than in our empirical networks (note that the blue line always ends in higher values of degree than the red one). This holds true both for the weighted interaction matrices generated by the model (where we obtain the cumulative distribution of strength) and for the unweighted version of the interaction matrix (where we obtain the cumulative degree distribution, shown in Fig. S11), that we use to generate the effective interaction matrices (α').

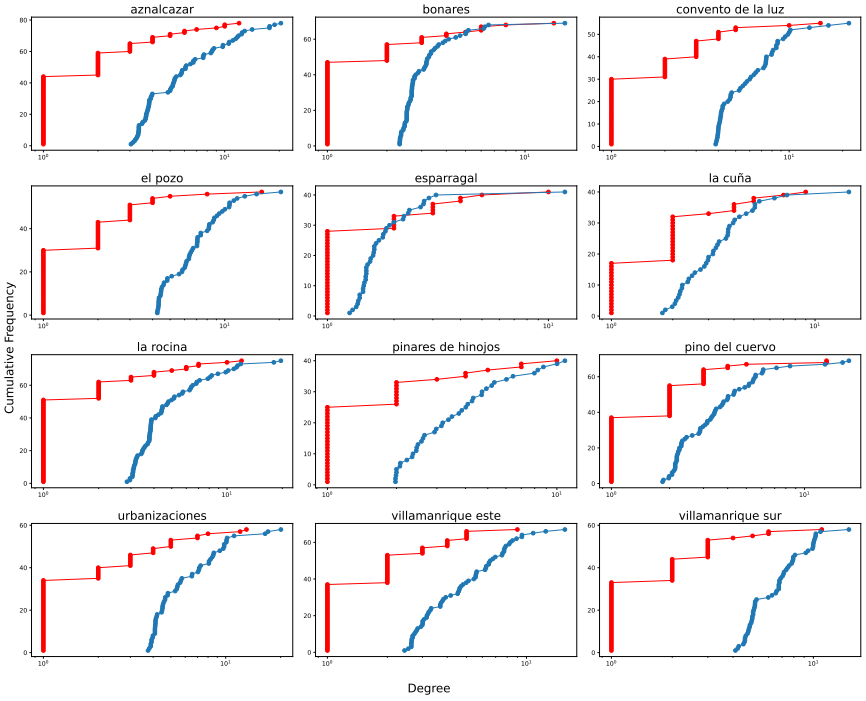

Figure S11: Cumulative degree distribution of the different plant-pollinator interaction networks in our study, showing the empirical distribution (in red) and the average distribution of 100 networks using null model of Vazquet et al.

Figure S12 shows the comparative of the weighted interaction empirical matrices (odd rows) with one randomization using the null model (even rows). Note that the randomized matrices have the interactions more spread through all species pairs than in the case of empirical matrices.

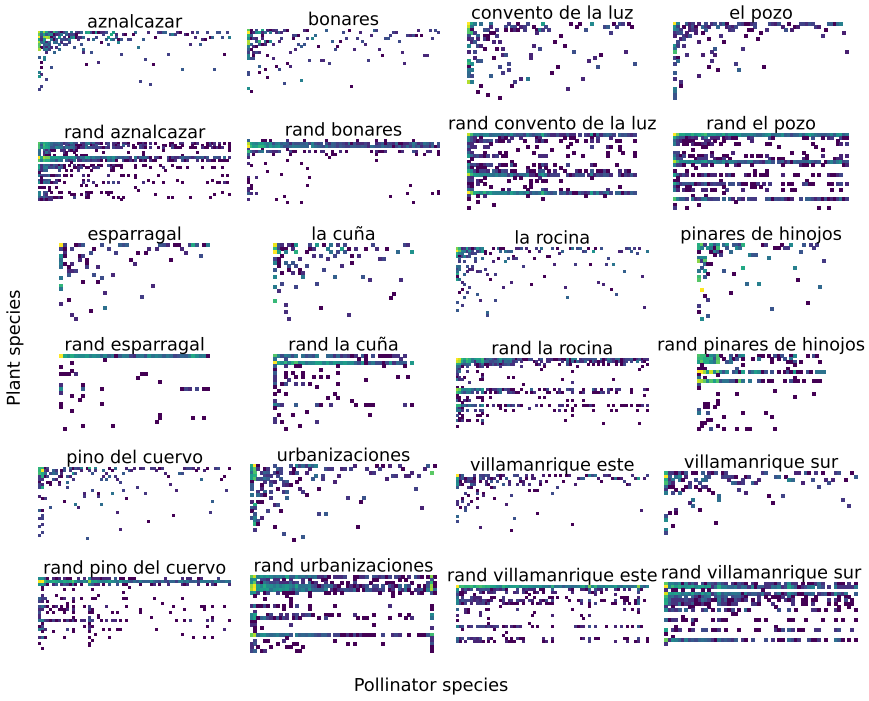

Figure S12: Weighted interaction empirical matrices (odd rows) and their randomized counterparts using the null model of Vazquez et al. (even rows). The color or the square represents the interaction frequency, whereas lighter tones represent a higher interaction frequency, and is in logarithmic scale.

While the degree distributions were not similar, null networks still showed realistic nested patterns (Fig. S12) in line with previous results [5]. Hence, we decided to go one step forward and compare the predicted probability of persistence using as the mutualistic interaction matrix (γ) the randomized version of our empirical mutualistic matrices obtained from the field observation (Fig. .S13). As can be seen, the expected persistence probability (ω_i) obtained using the randomized counterparts of the empirical mutualistic matrices (in black) does not capture the positive trend we find when using the empirical mutualistic matrix (in blue), clarifying that the abundances of species alone are not driving the expected persistence probabilities. Hence, persistent networks not only need to be nested, but also show specific degree distributions depicting who interacts with whom.

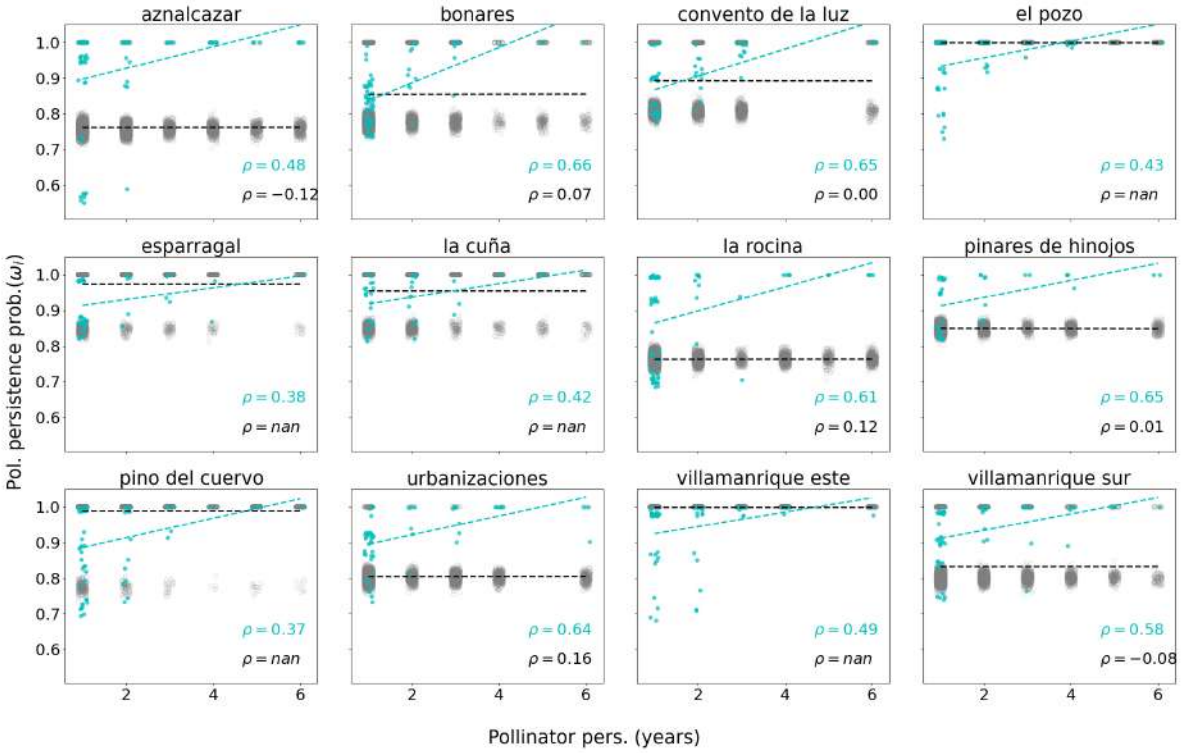

Figure S13: Pollinator persistence probability vs pollinator persistence in the field for each study site. The figure shows the results of the theoretical model using the empirical interaction network (in blue) compared with the results of 100 random realizations (right). Each point represents one species in the community, the dotted lines represent the linear regression that better fits the point for the empirical result (blue), or the mean of the randomizations (black). Spearman's correlation coefficients are shown in each figure (ρ). Note that black points in the upper part of the figures correspond to random interaction matrices of communities where all species are expected to survive (ω_i=1).

10 Role of abundance in determining temporal stability

We have confirmed that the exponent of the Taylor's Law between the logarithm of the variance of abundance and the logarithm of the mean abundance is equal to 2 (Fig. S14), meaning that we can use the CV (or its inverse) to quantify the temporal stability of the populations [6] because it will not be mainly driven by abundance.

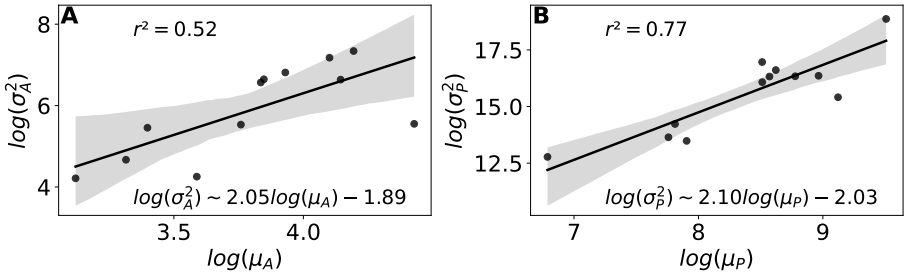

Figure S14: Variance of abundances vs mean abundances for A) pollinators and B) plants. The inline equation is the best fit of the linear regression, and the r^2 of the models are shown in the upper part of the figure. The shaded areas represent the 95% confidence interval of the regression estimates.

We directly checked that the temporal stability was not simply determined by mean abundance (Fig. R.S15, even if this was expected given the relationship shown in Fig. S14).

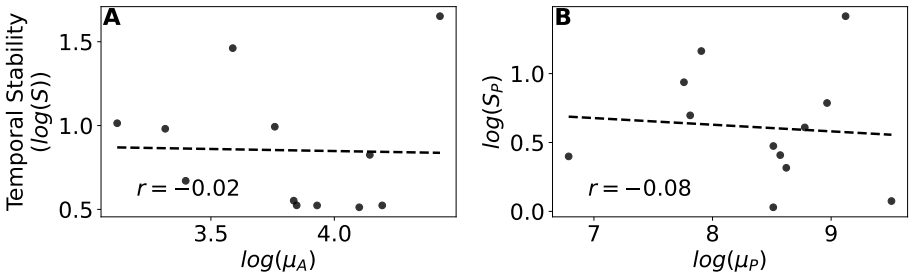

Figure S15: Temporal stability vs mean abundance for A) pollinators and B) plants. Each point represents a study site. The dashed lines represent the linear regression of the best-fitted model. Pearson's correlation coefficient appears in each figure.

We also checked whether the metric of population synchrony (η) was driven by the mean abundance but we did not find such a relationship (Fig. .S16).

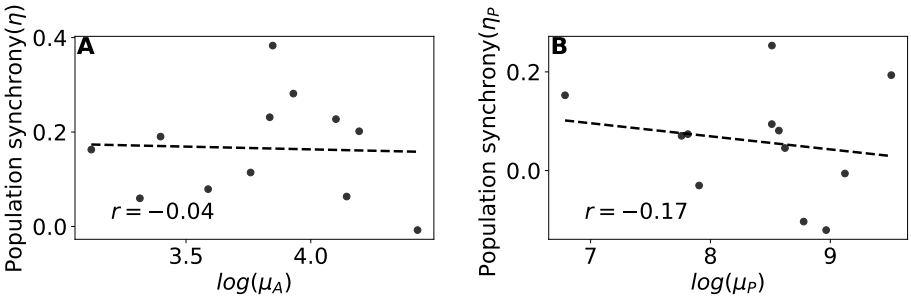

Figure S16: Population Synchrony vs mean abundance for A) pollinators and B) plants. Each point represents a study site. The dashed lines represent the linear regression of the best-fitted model. Pearson's correlation coefficient appears in each figure.

11 Structural features determining Structural stability

Since comparing the empirical networks with their randomized counterparts in the null model of Vázquez et al (null model "A") shows that some empirical networks are more structurally stable than their randomizations, while other are less, we decided to further study the structural drivers of the structural stability of the empirical networks. In order to disentangle what basic structural features were driving the enhanced stability in empirical networks, we implemented three other null models with increasing constraints, and compared the structural stability of the empirical networks with that of their randomized versions.

The first and most simple null model, the Erdös-Rényi model (hereon named "B") keeps constant the number of species in each species set (i.e. plants and pollinators) and the number of interactions and connectance. If a feature measured in the empirical network and in this random ensemble coincide, it means that it is network size and connectance what is driving that feature. Next, we implemented the configuration model (hereon named "C") that adds the constraint of keeping also the degree distribution. If a feature measured in the empirical network and in this ensemble coincide, but they do not in the previous ensemble, it means that it is not size and connectance what is driving this feature, but the degree heterogeneity. Note that while the original configuration model allows the existence of multiple links between a pair of species, we forbid this, meaning that the resulting network may slightly deviate from the original degree sequence, but will maintain the general form of the degree distribution. We implemented the configuration model using the function *configuration_model* from the *bipartite* section in Python's *networkx*[7]. Finally, we implemented the most constrained null model (hereon named "D") where we keep constant the particular degree sequence of the empirical network but reshuffle the interactions. If a feature measured in the empirical network does not coincide in the randomized ensemble B and C, but it does coincide in the randomized ensemble D it means that it is the particular degree sequence of the empirical network what is driving that feature (i.e. we need almost all the information of how the network is connected in order to understand the feature we are interested in). We implemented this null model using the curveball algorithm [8] to avoid bias in the sampling of the randomized networks.

When we look at the empirical networks, and compare them with their randomizations in the 4 new null models (A to D), we can better understand what is driving structural stability in the empirical networks (see Fig. S17). While when compared with their randomizations in null model A (panel A) the empirical networks can have either higher or lower average persistence probability (ω), when we keep the connectance constrained in null model B, we find that in all cases the empirical value of ω is much higher than what is found in the randomized networks (panel B). This clarifies that while connectance is important, how these connection are distributed matters even more. This means that it is possible to have more connectance and still be less structurally stable than other networks with lower connectance but a different connection pattern. In order to study how the network is connected, is usual to look at the degree distribution . While considering networks with a similar degree distribution helps in order to enhance the structural stability, as shown in the comparison with null model C (panel C in Fig. S17), still the empirical networks in the example seem to have degree sequences that are not easy to get in their randomized counterparts. Finally, it is only when we use the most constrained null model, D, that the average persistence probability (ω) in the empirical and randomized networks are similar (panel D), pointing to the relevance of the particular degree sequence in determining the structural stability of the ecological community.

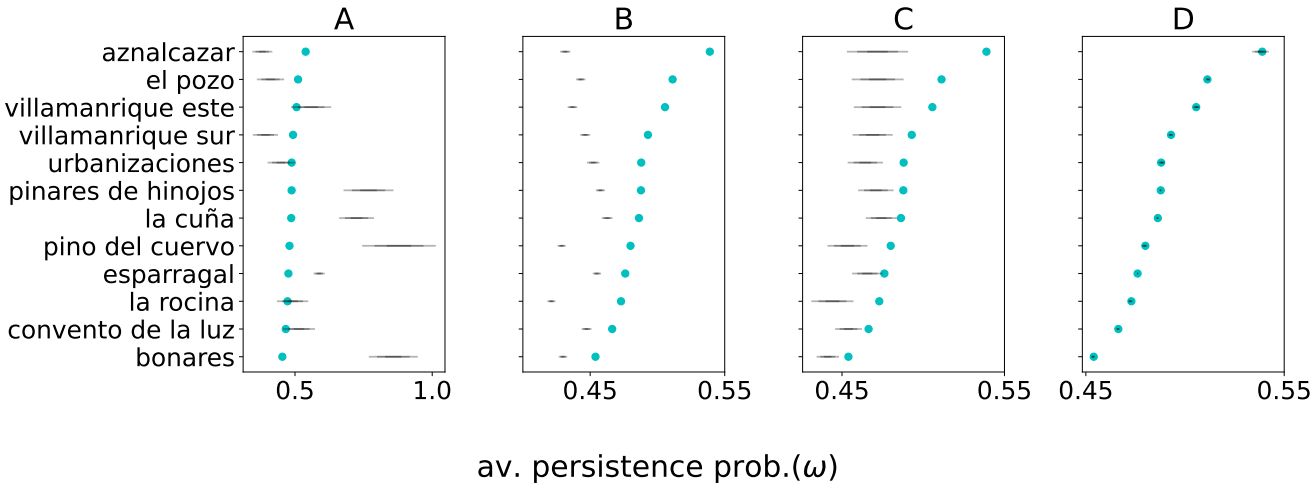

Figure S17: Comparative of the average pollinator persistence probability (ω) obtained using the empirical network (blue dots) with the values obtained using their randomizations in 4 different null models (A to D, one in each column) in all the study sites. The black-shaded intervals represent one, two, and three standard deviations, and are centered at the average value obtained in 100 randomizations.

12 Parameter robustness

In order to check the robustness of our results, we repeated the first analysis (correlation of empirical persistence versus average expected persistence probability (ω)) with different values for the dynamical parameters of intra-guild competition (α), average mutualistic gain (γ_0), and mutualistic trade-off (δ). The different values of γ_0 explored are those compatible with the linear stability of the least stable system (i.e., those below the minimum γ_0 threshold)[1]. The results are summed up in Table S2. In the main text we used α=0.005, γ_0=0.1, and $\delta = 0$, similarly as in previous studies[1]. Looking at the table we can see that as long as the mutualistic strength is large enough for a given competition strength, the correlation appears. In the cases where competition is higher, we did not check larger values of γ_0 because we choose the same value for all the networks in the database, and hence we were limited by the threshold value of the least stable network, but we guess that if the increase the mutualistic gain value for the networks that are stable we will recover that high empirical persistence is associated with a high predicted average probability of persistence.

References

[1] Saavedra, S., Rohr, R. P., Olesen, J. M. & Bascompte, J. Nested species interactions promote feasibility over stability during the assembly of a pollinator community. *Ecology and Evolution* **6**, 997–1007 (2016).

[2] Jonhson, S., Domínguez-García, V. & Muñoz, M. A. Factors determining nestedness in complex networks. *PLoS ONE* **8**, e74025 (2013).

[3] Rohr, R. P., Saavedra, S. & Bascompte, J. On the structural stability of mutualistic systems. *Science* **345**, 1253497–1253497 (2014).

[4] Vázquez, D. P. *et al.* Species abundance and asymmetric interaction strength in ecological networks. *Oikos* **116**, 1120–1127 (2007).

[5] Olito, C. & Fox, J. W. Species traits and abundances predict metrics of plant-pollinator network structure, but not pairwise interactions. *Oikos* **124**, 428–436 (2014).

[6] Reckling, M. *et al.* Methods of yield stability analysis in long-term field experiments. a review. *Agron. Sustain. Dev.* **41** (2021).

[7] Hagberg, A., Swart, P. & S Chult, D. Exploring network structure, dynamics, and function using networkx. Tech. Rep., Los Alamos National Lab.(LANL), Los Alamos, NM (United States) (2008).

[8] Strona, G., Nappo, D., Boccacci, F., Fattorini, S. & San-Miguel-Ayanz, J. A fast and unbiased procedure to randomize ecological binary matrices with fixed row and column totals. *Nature Communications* **5** (2014).

α	γ_0	δ	ρ (Plants)	ρ (Pollinators)
0.001	0.10	0.0	0.81	0.66
		0.2	0.82	0.69
		0.5	0.82	0.74
		0.7	0.81	0.77
	0.11	0.0	0.79	0.63
		0.2	0.81	0.67
		0.5	0.82	0.71
		0.7	0.82	0.74
	0.12	0.2	0.79	0.65
		0.5	0.82	0.70
		0.7	0.82	0.72
	0.13	0.5	0.82	0.68
		0.7	0.82	0.71
	0.14	0.5	0.82	0.67
		0.7	0.82	0.69
	0.15	0.5	0.81	0.66
		0.7	0.82	0.68
0.002	0.10	0.0	0.83	0.71
		0.2	0.83	0.75
		0.5	0.80	0.83
		0.7	0.77	0.85
	0.11	0.0	0.82	0.67
		0.2	0.83	0.71
		0.5	0.82	0.79
		0.7	0.78	0.84
	0.12	0.2	0.82	0.68
		0.5	0.82	0.76
		0.7	0.80	0.81
	0.13	0.5	0.83	0.74
		0.7	0.81	0.78
	0.14	0.5	0.83	0.71
		0.7	0.81	0.76
	0.15	0.5	0.83	0.69
		0.7	0.82	0.74
0.003	0.10	0.0	0.83	0.77
		0.2	0.81	0.81
		0.5	0.77	0.88
		0.7	0.72	0.72
	0.11	0.0	0.83	0.71
		0.2	0.82	0.76
		0.5	0.79	0.86
		0.7	0.74	0.81
	0.12	0.2	0.83	0.72
		0.5	0.80	0.83
		0.7	0.76	0.84
	0.13	0.2	0.82	0.69
		0.5	0.81	0.79
		0.7	0.77	0.84
	0.14	0.5	0.82	0.76
		0.7	0.79	0.82
	0.15	0.5	0.82	0.73
		0.7	0.80	0.79
0.005	0.10	0.0	0.79	0.85
		0.2	0.76	0.87
		0.5	0.70	0.68
		0.7	0.65	0.35
0.005	0.11	0.0	0.80	0.81
		0.2	0.78	0.85
		0.5	0.72	0.81
		0.7	0.67	0.48
	0.13	0.2	0.81	0.75
		0.5	0.76	0.87
		0.7	0.70	0.73
	0.14	0.5	0.78	0.84
		0.7	0.72	0.80
	0.15	0.5	0.79	0.81
		0.7	0.74	0.83
0.010	0.10	0.0	0.69	0.57
		0.2	0.66	0.46
		0.5	0.61	0.21
		0.7	0.57	0.07
	0.11	0.0	0.71	0.72
		0.2	0.68	0.63
		0.5	0.62	0.30
		0.7	0.58	0.12
	0.12	0.0	0.72	0.82
		0.2	0.70	0.76
		0.5	0.64	0.41
		0.7	0.59	0.18
	0.13	0.0	0.67	0.86
		0.2	0.72	0.84
		0.5	0.65	0.55
		0.7	0.60	0.25
	0.14	0.2	0.72	0.85
		0.5	0.67	0.68
		0.7	0.61	0.33
	0.15	0.5	0.68	0.78
		0.7	0.62	0.42
0.020	0.10	0.0	0.63	0.14
		0.2	0.59	0.03
		0.5	0.57	0.03
		0.7	0.51	0.06
	0.11	0.0	0.61	0.20
		0.2	0.61	0.16
		0.5	0.56	0.06
		0.7	0.52	0.02
	0.12	0.0	0.61	0.33
		0.2	0.58	0.21
		0.5	0.55	0.12
		0.7	0.52	0.02
	0.13	0.0	0.60	0.39
		0.2	0.62	0.35
		0.5	0.57	0.14
		0.7	0.54	0.02
	0.14	0.0	0.59	0.46
		0.2	0.60	0.39
		0.5	0.59	0.17
		0.7	0.55	0.05
	0.15	0.2	0.61	0.52
		0.5	0.57	0.23
		0.7	0.52	0.14

Table S2: Correlation between empirical persistence and average expected persistence probability (ρ), for plants and pollinators, as a function of the dynamical parameters of the mutualistic model: intra-guild mean-field competition (α), average mutualistic gain(γ_0), and mutualistic trade-off (δ).